On-line Finger-Knuckle-Print Identification Using Gaussian Mixture Models & Discrete Cosine Transform

Abdallah Meraoumia[1],Salim Chitroub[2] and Ahmed Bouridane[3,4]

[1]Kasdi Merbah university of Ouargla, Electrical engineering Laboratory
Sciences and Technology and Mater Sciences Faculty, Ouargla, 30000, Algeria
[2]Signal and Image Processing Laboratory, Electronics and Computer Science Faculty, USTHB.
P.O. box 32, El Alia, Bab Ezzouar, 16111, Algiers, Algeria
[3]School of Computing, Engineering and Information Sciences, Northumbria University,
Pandon Building, Newcastle upon Tyne, UK.
[4]Department of Computer Science, King Saudi University,
P.O. Box 2454, Riyadh, 11451, Saudi Arabia
Email: Ameraoumia@gmail.com, S_chitroub@hotmail.com, Ahmed.Bouridane@northumbria.ac.uk, ABouridane.c@ksu.edu.sa

***Abstract*—Biometric system has been actively emerging in various industries for the past few years, and it is continuing to roll to provide higher security features for access control system. In the recent years, hand based biometrics is extensively used for personal recognition. In this paper, we propose an efficient online personal identification system based on Finger-Knuckle-Print (FKP) using the Gaussian Mixture Model (*GMM*) and two-dimensional Block Based Discrete Cosine Transform (*2D-BDCT*). In this study, a segmented *FKP* is firstly divided into non-overlapping and equal-sized blocks, and then, applies the *2D-BDCT* over each block. By using zigzag scan order each transform block is reordered to produce the feature vector. Subsequently, we use the *GMM* for modeling the feature vector of each FKP. Finally, Log-likelihood scores are used for FKP matching. Experimental results show that our proposed method yields the best performance for identifying FKPs and it is able to provide an excellent identification rate and provide more security.**

***Index Terms*—Biometrics, identification, Finger-Knuckle-Print, *2D-BDCT*, *GMM*, Data fusion.**

I. INTRODUCTION

PERSONAL identification plays a critical role in our society. Traditional knowledge based or token-based personal identification systems are time-consuming, inefficient and expensive. Biometrics offers a natural and reliable solution to the problem of identity determination by recognizing individuals based on some characteristics that are inherent to the person [1]. Biometrics is a study of methods for uniquely recognizing individuals based on one or more intrinsic physical or behavioral traits, including the extensively studied fingerprint, iris, speech, hand geometry, and palmprint. One of the most popular biometric systems is based on the hand due to its ease of use. Recently, a novel hand-based biometric feature, finger-knuckle-print (FKP), has attracted an increasing amount of attention [2]. The texture pattern produced by the finger knuckle bending is highly unique and makes the surface a distinctive biometric identifier. Like any other biometric identifiers, FKPs are believed to have the critical properties of universality, uniqueness, and permanence for personal recognition [3].

An important issue in FKP identification is to extract FKP features that can discriminate an individual from the other. Based on texture analysis, our biometric identification system used the 2D-BDCT for features extracted from FKP images. In this method, a FKP is firstly divided into non-overlapping and equalized blocks, and then, applies the 2D discrete cosine transform over each block. By using zigzag scan order, each transform block is reordered to produce the feature vector and then concatenated all vectors for produce an observation vector. Subsequently, we use the *GMM* for modeling this vector (for each FKP). Finally, log-likelihood scores are used for matching. In this work, a series of experiments were carried out using a FKP database. To evaluate the efficiency of this technique, the experiments were designed as follow: the performances under different finger types were compared to each other, in order to determine the best finger type at which the FKP identification system performs. However, because our database contains FKPs from four types of fingers, an ideal FKP identification system should be based on the fusion of these fingers at different fusion levels.

The rest of the paper is organized as follows: The proposed FKP recognition scheme is presented in section 2. Section 3 gives a brief description of the method used for extracting the Region Of Interest (*ROI*). The feature extraction and modeling process, including an overview of the two-dimensional block based discrete cosine transform and the gaussian mixture model, is presented in section 4. A sections 5 is devoted to describe the evaluation and normalization method. The obtained results, prior to fusion and after fusion, are evaluated and commented in section 6. Finally, conclusions and future work are given in section 7.

II. SYSTEM OVERVIEW

Fig. 1 illustrates the various modules of our proposed unimodal FKP identification system (single finger). The proposed system consists of preprocessing, feature extraction and modeling, matching and decision stages. To enroll into the system database, the user has to provide a set of training FKP images. Typically, an observation vector is extracted from each finger which describes certain characteristics of the FKP images using Discrete Cosine Transform (*DCT*) technique and modeling using gaussian mixture model. Finally, the models parameters are stored as references models. For identification, the same observation vectors are extracted from the test FKP images and the log-likelihood is computed using all of models

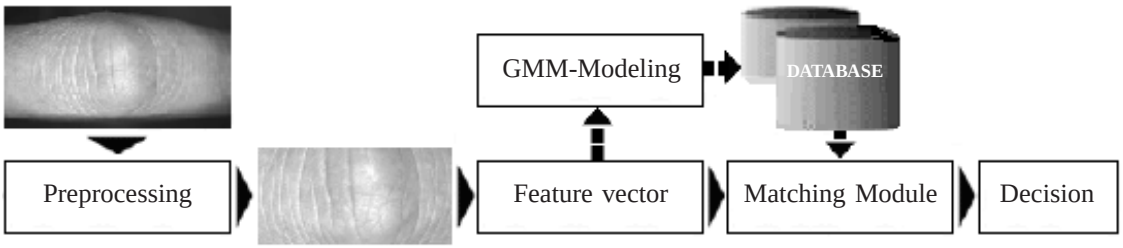

Fig. 1. Block-diagram of the FKP identification system based on the gaussian mixture model.

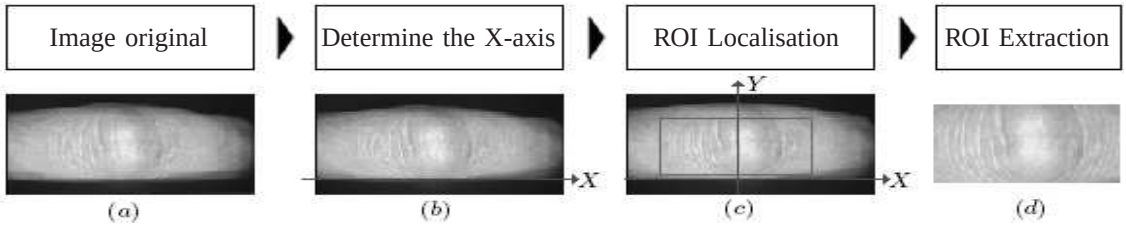

Fig. 2. ROI extraction process. (a) Image original; (b) X-axis of the coordinate system; (c) ROI coordinate system and (d) Region of interest (ROI)

references. Our database contains FKPs from four types of fingers, for this raison, each FKP modalities are used as inputs of the matcher modules (sub-system). For the multi-modal system, each sub-system compute its own matching score and these individual scores are finally combined into a total score (using fusion at the matching score level), which is used by the decision module. We have also tried the fusion at the decision level to choose the best one for FKPs classification.

III. Region of interest extraction

After the image is captured, it is pre-processed to obtain only the area information of the FKP. The detailed steps for pre-processing process are as follows [4]: First, apply a Gaussian smoothing operation to the original image. Second, determine the X-axis of the coordinate system fitted from the bottom boundary of the finger; the bottom boundary of the finger can be easily extracted by a Canny edge detector. Third, determine the Y-axis of the coordinate system by applying a Canny edge detector on the cropped sub-image extracted from the image original base on X-axis, then find the convex direction coding scheme. Finally, extract the *ROI* coordinate system, where the rectangle indicates the area of the *ROI* that will be extracted. The pre-processing steps are shown in Fig. 2.

IV. Feature extraction and modeling

A. 2D Block based discrete cosine transform

Discrete cosine transform is a powerful transform to extract proper features for FKP identification. The *DCT* is the most widely used transform in image processing algorithms, such as image/video compression and pattern recognition. Its popularity is due mainly to the fact that it achieves a good data compaction, that is, it concentrates the information content in a relatively few transform coefficients [5]. In the *2D-BDCT* formulation, the input image is first divided into $\eta_1 \times \eta_2$ blocks, and the *2D-DCT* of each block is determined. The 2D-*DCT* can be obtained by performing a *1D-DCT* on the columns and a *1D-DCT* on the rows. Given an image f, where H, W represent their size, the *DCT* coefficients of the spatial block are then determined by the following formula:

$$F_{ij}(u,v) = C(v)C(u) \sum_{m=0}^{M-1} \sum_{n=0}^{M-1} f_{ij}(n,m)\psi(n,m,u,v) \qquad (1)$$

$$\psi(n,m,u,v) = \cos\left[\frac{(2n+1)u\pi}{2M}\right] \cos\left[\frac{(2m+1)v\pi}{2M}\right] \qquad (2)$$

$u, v = 0, 1, \cdots, M-1$, $i = 1, \cdots, \eta_1$, $j = 1, \cdots, \eta_2$ with $\eta_1 = \frac{H}{M}$, $\eta_2 = \frac{W}{M}$ and $F_{ij}(u,v)$ are the DCT coefficients of the B_{ij} block, $f_{ij}(n,m)$ is the luminance value of the pixel (n,m) of the B_{ij} block, and

$$C(u) = \begin{cases} \frac{1}{\sqrt{2}} & \text{if} \quad u = 0 \\ 1 & \text{if} \quad u \neq 0 \end{cases} \qquad (3)$$

After transformation process, if *M=8*, there will be 64 *DCT* coefficients contained within each transformed block, where the coefficient at the top-left is called DC $\langle F_{ij}(0,0) \rangle$ coefficient and the rest is called AC coefficients.

B. Observation vector

The block-based approach partitions the input image, with size $H \times W$, when $H = 220$ and $W = 110$, into small non-overlapped blocks; each of them is then mapped into a block of coefficients via the *2D-DCT*. Most popular block size is commonly set to $M \times M$ with *M=8*. The number of blocks extracted from each FKP image equals to:

$$\eta = \lfloor \eta_1 \rfloor * \lfloor \eta_2 \rfloor = \lfloor \frac{220}{8} \rfloor * \lfloor \frac{110}{8} \rfloor = 27 * 13 = 351 \text{ blocks} \qquad (4)$$

Then, we form a feature vector from the *2D-DCT* coefficients of each image block (see Fig. 3). The *2D-DCT* concentrates the information content in a relatively few transform coefficients top-left zone of block, for this, the coefficients, where the information is concentrated, tend to be grouped together at the start of the reordered array, Thus, a suitable scan order is a zigzag starting from the DC (top-left) coefficient [6]. Starting

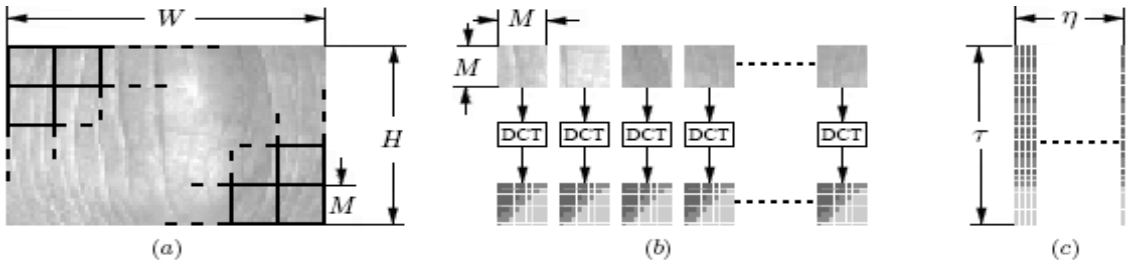

Fig. 3. Observation vector extraction. *(a)* blocks extraction, *(b)* block feature extraction and *(c)* Observation vector.

with the DC coefficient, each coefficient is copied into a one-dimensional array. So, each block can be represented by a vector of coefficients:

$$O_{ij} = [F_{ij}(0,0) \quad F_{ij}(0,1) \quad F_{ij}(1,0) \cdots\cdots F_{ij}(U,V)]^T \tag{5}$$

U, V are chosen as well as the identification rate was maximum. Thus, $U, V \in [0 \cdot\cdot 7]$ and the size of O_{ij} is τ with $\tau \in [1 \cdot\cdot 64]$. Finally, the results o_{ij} of a blocks image are combined in the single template as follows:

$$V_{Obs} = [O_{11} \quad O_{12} \quad O_{13} \quad O_{14} \cdots O_{\eta_1 \eta_2}] \tag{6}$$

Where the size of resulting observation vector is $[\tau \quad \eta]$.

C. Gaussian mixture model

Gaussian mixture model is pattern recognition technique that uses an approach of the statistical methods [7]. The observation vector of each class measurement can be described by normal distribution, also called Gaussian distribution. Each class measurement may be then defined by two parameters: mean (average) and standard deviation (variability). Suppose that the observation vector is the discrete random variable V_{Obs}. For the general case, where vector is multidimensional, the probability density function of the normal distribution is a gaussian function:

$$P(V_{Obs}|\mu, \Sigma) = \frac{1}{\sqrt{(2\pi)^d |\Sigma|}} \exp\left[-\frac{1}{2}(V_{Obs} - \mu)^T \Sigma^{-1} (V_{Obs} - \mu)\right] \tag{7}$$

where μ is the mean, Σ is the covariance matrix and d is the dimension of feature vector. Covariance matrix is the natural generalization to higher dimensions of the concept of the variance of a random variable. If we suppose the random variable measurement is not characterized only with simple gaussian distribution, we can then define it with multiple gaussian components. *GMM* is a probability distribution that is a convex combination of other gaussian distributions:

$$P(V_{Obs}) = \sum_{j=1}^{N} \pi_j P(V_{Obs}|\mu_j, \Sigma_j) \tag{8}$$

where N is the number of Gaussian mixtures and π_j is the weight of each of the mixture. After *GMM* is trained, the model of each user will be the final values of π_j, μ_j and Σ_j. Thus, the compact notation θ, such that $\theta = \{\pi_j, \mu_j, \Sigma_j\}_{j=1}^{N}$, is used to represent a model. To estimate the density parameters of a *GMM* statistic model, cluster estimation method called Expectation-maximization algorithm (EM) is adopted. The EM is the ideal candidate for solving parameter estimation problems for the *GMM*. Each of the EM iterations consists of two steps Estimation (E) and Maximization (M). The M-step maximizes a likelihood function that is refined in each iteration by the E-step.

V. Feature matching and normalization

After extracting the observation vectors corresponding to the test images, the probability of the observation sequence given a GMM model is computed. The model with the highest log-likelihood is selected and this model reveals the identity of the unknown finger. Thus, during the identification process, the characteristics of the test image are extraction by the *2D-BDCT* corresponding to each person. Then the Log-likelihood score of the observation vectors given each model, $P(V_{Obs}|\theta_i) = \ell(V_{Obs}, \theta_i)$, is computed [8]. Therefore, the score vector is given by:

$$\mathfrak{L}(V_{Obs}) = [\ell(V_{Obs}, \theta_1) \quad \ell(V_{Obs}, \theta_2) \cdots \ell(V_{Obs}, \theta_D)] \tag{9}$$

Where D represents the size of model database.

An important aspect that has to be addressed in identification process is the normalization of the scores obtained. Normalization typically involves mapping the scores obtained into a common domain. Thus, a *Min-Max* normalization scheme was employed to transform the Log-likelihood scores computed into similarity scores in the same range.

$$\mathfrak{L}_N = \frac{\mathfrak{L} - min(\mathfrak{L})}{max(\mathfrak{L}) - min(\mathfrak{L})} \tag{10}$$

Where $\mathfrak{L}_N$ denotes the normalized Log-likelihood scores. However, these scores are compared, and the highest score is selected. Therefore, the best score is D_o and its equal to:

$$D_o = \max_i(\mathfrak{L}_N) \tag{11}$$

Finally, this score is used for decision making.

VI. Experimental results and discussion

A. Experimental database

We experimented our method on Hong Kong polytechnic university (PolyU) FKP Database [9]. The database has a total of 7920 images obtained from 165 persons. this database including 125 males and 40 females. Among them, 143 subjects are 20∼30 years old and the others are 30∼50 years old. these images are collected in two separate sessions. In each session, the subject was asked to provide 6 images for each of Left Index Fingers (LIF), Left Middle Fingers (LMF), Right Index Fingers (RIF) and Right Middle Fingers (RMF). Therefore, 48 images were collected from each subject.

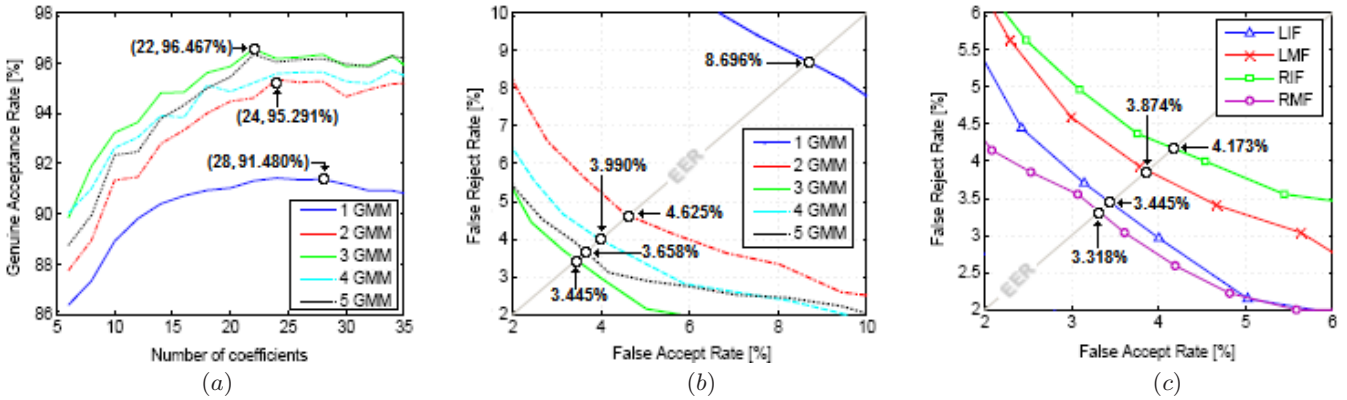

Fig. 4. Uni-modal open set identification system performance. *(a)* System performance under different *2D-BDCT* coefficients number in each block and various *GMM*, *(b)* The ROC curves for all GMMs and *(c)* The ROC curves for all finger types.

TABLE 1 : OPEN SET IDENTIFICATION TEST RESULT IN THE CASE OF UNI-MODAL SYSTEM

DATABASE	LEFT INDEX FINGER			LEFT MIDDLE FINGER			RIGHT INDEX FINGER			RIGHT MIDDLE FINGER		
	T_o	FAR	FRR	T_o	*FAR*	FRR	T_o	FAR	FRR	T_o	FAR	FRR
	0.9600	8.808	1.556	0.9600	7.970	1.630	0.6500	8.777	2.963	0.9400	7.820	1.482
165 Persons	0.9740	3.445	3.445	0.9717	3.874	3.874	0.9644	4.173	4.173	**0.9586**	**3.318**	**3.318**
	0.9850	1.158	7.630	0.9800	1.866	6.593	0.9800	1.332	7.630	0.9800	0.731	7.259

B. Evaluation criteria

The measure of utility of any biometric recognition system for a particular application can be explained by two values [10]. The value of the False Acceptance Rate (FAR) criterion, which is the ratio of the number of instances of different feature pairs of the traits found do match to the total number of counterpart attempts, and the value of the False Rejection Rate (*FRR*) criterion, which is the ratio of the number of instances of same feature pairs of the traits found do not match to the total number of counterpart attempts. It is clear that the system can be adjusted to vary the values of these two criteria for a particular application. However, decreasing one involves increasing the other and vice versa. The system threshold value is obtained using Equal Error Rate (*EER*) criteria when *FAR* = *FRR*. This is based on the rationale that both rates must be as low as possible for the biometric system to work effectively. Another performance measurement is obtained from *FAR* and *FRR*, which is the Genuine Acceptance Rate (*GAR*). It represents the identification rate of the system. In order to visually describe the performance of a biometric system, Receiver Operating Characteristics (ROC) curves are usually given. A ROC curve shows how the FAR values are changed relatively to the values of the GAR and vice-versa [11]. Biometric recognition systems generate matching scores that represent the degree of similarity (or dissimilarity) between the input and the stored template.

C. 2D-BDCT coefficients selection in each block

The *2D-BDCT* coefficients reflect the compact energy of different frequencies. Most of the higher frequency coefficients are small and they become negligible, as result, the features derived from the *2D-BDCT* computation is limited to an array of summed spectral energies within a block in frequency domain. In this section, we present the identification accuracy of our system as a function of the number of *2D-BDCT* coefficients (in each block) used. The performance evaluation was repeated for various numbers of *2D-BDCT* coefficients and various numbers of *GMM*, and the results are as shown in Fig. 4.*(a)*. The reason Fig. 4.*(a)* was generated was to show how the number of *2D-BDCT* coefficients selection in each block and the number of *GMMs* used might have an effect on the performance of our system. We observe that the identification accuracy becomes very high at certain coefficients and slight decrease in identification accuracy as we go to higher numbers of coefficients. For example, if *1-GMM* with 28 coefficients in each block, is used for the identification, we have a GAR equal to 91.480 %. In the case of using *2-GMM* with 24 coefficients in each block, GAR was 95.291 %. *3-GMM* with 22 coefficients in each block, improves the result (GAR = 96.467 %) for a database size equal to 165 persons. In Fig. 4.*(b)*, we compare the system performance under different *GMMs*. The results show the benefits of using *3-GMM*. Thus, the performance of the open set uni-modal identification system is significantly improved by using the *3-GMM* with 22 coefficients in each block.

D. Uni-modal system test results

To evaluate the efficiency of the uni-modal biometric method, the experiments were designed as follow: three samples (for each finger) of each person is randomly selected for enrollment, and the rest nine finger images are used as test samples for identification. Thus, 123255 comparisons were generated for performance evaluation (165 persons). In this section we compare the performance of all finger types. In the case of open set identification, Fig. 4.*(c)* compares the performance of the system for deferent finger types. It can safely be see the benefits of using the RMF finger than the LIF, LMF and RIF fingers in terms of *EER*. It can be achieve an

TABLE 2 : OPEN SET IDENTIFICATION TEST RESULT IN THE CASE OF THE FUSION AT MATCHING SCORE LEVEL

COMBINATION	SUM		WHT		MIN		MAX		MUL	
	T_o	EER	T_o	EER	T_o	EER	T_o	EER	T_o	EER
LIF-LMF	0.9795	1.108	0.9795	1.115	0.9876	1.601	0.9723	1.562	0.9596	1.092
LIF-RIF	0.9735	1.519	0.9749	1.333	0.9851	1.874	0.9642	2.177	0.9483	1.489
LMF-RMF	0.9708	1.482	0.9701	1.510	0.9848	1.512	0.9627	1.770	0.9434	1.442
RIF-RMF	0.9664	1.577	0.9672	1.466	0.9833	1.447	0.9568	2.000	0.9354	1.556
All Fingers	0.9791	0.376	0.9792	0.375	0.9964	0.869	0.9607	1.239	**0.9190**	**0.370**

TABLE 3 : OPEN SET IDENTIFICATION TEST RESULT IN THE CASE OF THE FUSION AT DECISION LEVEL

LIF-LMF-RIF			LIF-LMF-RMF			RIF-RMF-LIF			RIF-RMF-LMF			All Fingers		
FAR	FRR	GAR	FAR	FRR	GAR	FAR	FRR	GAR	FAR	FRR	GAR	FAR	FRR	GAR
2.341	1.111	97.676	2.470	0.815	97.552	**0.705**	**1.037**	**99.291**	1.047	1.333	98.949	2.997	2.074	97.016

EER equal to 3.318 % at the threshold T_o = 0.9586. Therefore, the system can achieve higher accuracy at the RMF finger compared with the other finger types. Finally, Table 1 shows the *FAR* and *FRR* with percentage using LIF, LMF, RIF and RMF at deferent thresholds.

E. Multi-modal system test results

A robust identification system may require fusion of several finger types for the reason that the limitation presented in one finger may be compensated by another finger. The goal of this experiment was to investigate the systems performance when we fuse information from several finger types of a person. In fact, at such a case the system works as a kind of multi-modal system with a single biometric trait but multiple units. Therefore, information presented by different biometrics (LIF, LMF, RIF and RMF) is fused to make the system efficient.

1) Fusion at matching score level: Fusion at the matching-score level is preferred in the field of biometrics because there is sufficient information content and it is easy to access and combine the matching scores [12]. At the matching score level fusion, the matching scores output by multiple matchers (sub-system) are integrated. In our system, different combinations of finger types and different fusion rules, such as *Sum-score* (*SUM*), *Min-score* (*MIN*), *Max-score* (*MAX*), *Mul-score* (*MUL*) and *Sum-weighting score* (*WHT*), were tested to find the combination that optimizes the system accuracy. Thus, to find the better of the all fusion rules and combinations, with the lowest *EER*, Table 2 tabulates *EER* for various combinations and fusion rules. As can be seen, the best result was obtained with the combination of all fingers and the fusion rule was *MUL* rule, it can achieve even higher precision, an *EER* of 0.370 % and a T_o of 0.9190. The performance of the open set identification system is significantly improved by using the fusion and it is comparable with other hand based biometrics, such as hand geometry and fingerprint identification [13], [14].

2) Fusion at decision level: Designing a suitable method of decision combinations is a key point for the ensembles performance. In this paper, a simplest method for the voting schemes, *plurality vote*, is used [15]. However, in this method, just count the number of decision for each class and assign the sample to the class that obtained the highest number of votes. Note that, the number of sub-systems should be above or equal to 3. For the evaluation of the system performance, in the case of multi-modal system based on decision level, a series of experiments were carried out using a different finger type combinations and the results are shown in Table 3. From Table 3, it can be seen that our identification system achieves a best performance when using RIF, RMF and LIF (*FAR* = 0.705 %, *FRR* = 1.037% and GAR = 99.291%).

Finally, in Fig. 5.*(a)*, we compare the performance of different systems (uni-modal and multi-modal based on fusion at matching score level). The results show the benefits of using the multi-modal system with matching score level fusion. Therefor, the distance distributions of genuine and imposter matchings obtained by the proposed scheme, if the all fingers are fused in the case of matching score level by *MUL* rule and the results expressed as a *FAR* and *FRR* depending on the threshold, are plotted in Fig. 5.*(b)* and Fig. 5.*(c)*, respectively.

VII. CONCLUSION AND FURTHER WORK

In this paper, a multi-modal biometric identification system, using FKP biometric, based on fusion of several biometric traits, four finger types, has been proposed. Fusion of these biometric traits is carried out at the matching score level and decision level. The proposed system use *2D-BDCT* for feature extracted, *GMM* for modeling and log-likelihood for matching process. To compare the proposed multi-modal system with the uni-modal systems, a series of experiments has been performed in the case of open set identification and it has been found that the proposed multi-modal system gives a considerable performance gain over the uni-modal systems. Our future work will focus on the performance evaluation in both phases (verification and identification) by using a large size database and integration of other biometric traits such as fingerprint or face to get the system performances with a high accuracy.

REFERENCES

[1] Arun A. Ross, K. Nandakumar and A. K. Jain, “Handbook of Multibiometrics”, Springer Science+Business Media, LLC, New York, 2006.
[2] Rui Zhao, Kunlun Li, Ming Liu, Xue Sun, “A Novel Approach of Personal Identification Based on Single Knuckle-print Image”, Asia-Pacific Conference on Information Processing, APCIP, 2009.
[3] Lin Zhang, Lei Zhang, and David Zhang, “Finger-Knuckle-Print Verification Based on Band-Limited Phase-Only Correlation”, CAIP 2009, LNCS 5702, pp. 141-148, 2009.
[4] L. Zhang, L. Zhang, D. Zhang, “Finger-knuckle-print: a new biometric identifier”, in: Proceedings of the ICIP09, 2009.

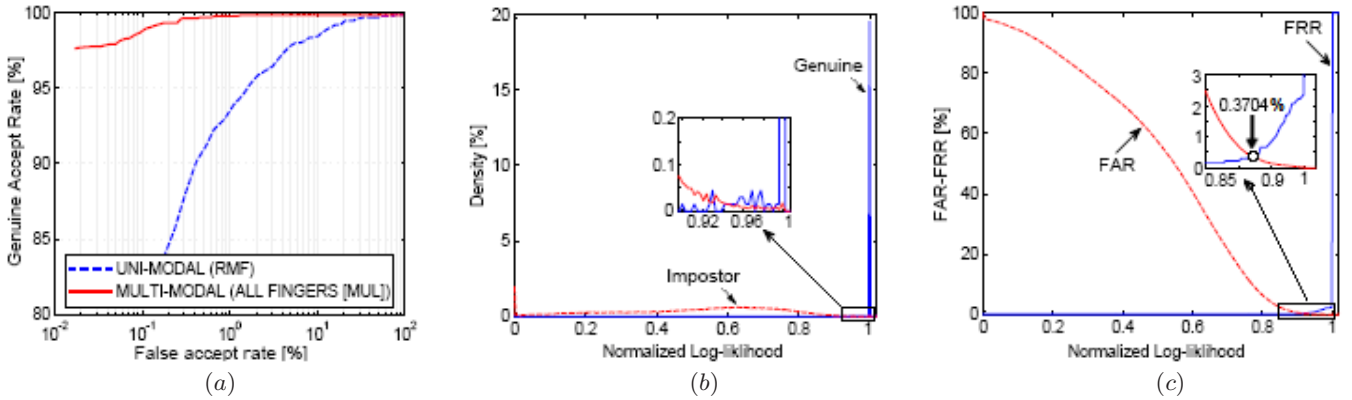

Fig. 5. Multi-modal system performance in the case of fusion at matching score level (all fingers) with *MUL* rule. *(a)* The comparison between the uni-modal and multi-modal systems, *(b)* The genuine and the imposter distribution and *(c)* The dependency of the *FAR* and the *FRR* on the value of the threshold.

[5] Ahmed N, Natarajan T, and Rao K, "Discrete cosine transform", IEEE Trans, on Computers, 23(1):9093.

[6] Abdallah Meraoumia, Salim Chitroub and Bouridane ahmed, "Gaussian Modeling And Discrete Cosine Transform For Efficient And Automatic Palmprint Identification", International Conference on Machine and Web Intelligence-ICMWI'2010, USTHB, Algiers, October 3-5, 2010.

[7] Peter Varchol, Dŭsan Levický, "Using of Hand Geometry in Biometric Security Systems", Radioengineering, VOL. 16, NO. 4, pp:82-87, December 2007

[8] Dimitrios Ververidis and Constantine Kotropoulos, "Gaussian mixture modeling by exploiting the Mahalanobis distance", IEEE Trans. Signal Processing, vol. 56, issue 7B, pp. 2797-2811, 2008.

[9] PolyU Finger KnucklePrint Database. Available: http://www4.comp.polyu.edu.hk/∼biometrics/ FKP.htm.

[10] Connie T., Teoh A., Goh M. and Ngo D, "Palmprint recognition with PCA and ICA", New Zealand, Palmerston North, 2003.

[11] Jain A. K. Ross, A. and Prabhakar, S, "An introduction to biometric recognition", IEEE Transactions on Circuits and Systems for Video Technology, 14(1), 420, 2004.

[12] Abdallah Meraoumia, Salim Chitroub and Ahmed Bouridane, "2D and 3D Palmprint Information and Hidden Markov Model for Improved Identification Performance", International conference on intelligent systems design and applications-ISDA 2011, Còrdoba, spain, November 22-24, 2011

[13] S. M. Prasad, V. K. Govindan, P. S. Sathidevi, "Palmprint Authentication Using Fusion of Wavelet Based Representations", Procedinng by IEEE, pp.520-525, 2009.

[14] Richa Singh, Mayank Vatsa, Afzel Noore, "Hierarchical fusion of multispectral face images for improved recognition performance", science direct, Information Fusion 9 (2008) 200-210.

[15] Francisco Moreno-Seco, José M. Iñesta, Pedro J. Ponce de León and Luisa Micó, "Comparison of classifier Fusion Methodes for Classification in Pattern Recognition Tasks", LNCS 4109, pp: 705-713, 2006.